Universität des Saarlandes

Fachrichtung 6.1 – Mathematik

Preprint Nr. 316

FEM with Trefftz trial functions on polyhedral elements

Sergej Rjasanow and Steffen Weißer

Saarbrücken 2012

Fachrichtung 6.1 – Mathematik
Universität des Saarlandes

Preprint No. 316
submitted: Oct 22, 2012

FEM with Trefftz trial functions on polyhedral elements

Sergej Rjasanow

Saarland University
Department of Mathematics
P.O. Box 15 11 50
66041 Saarbrücken
Germany
rjasanow@num.uni-sb.de

Steffen Weißer

Saarland University
Department of Mathematics
P.O. Box 15 11 50
66041 Saarbrücken
Germany
weisser@num.uni-sb.de

Edited by
FR 6.1 – Mathematik
Universität des Saarlandes
Postfach 15 11 50
66041 Saarbrücken
Germany

Fax: + 49 681 302 4443
e-Mail: preprint@math.uni-sb.de
WWW: http://www.math.uni-sb.de/

FEM with Trefftz trial functions on polyhedral elements

Sergej Rjasanow Steffen Weißer

October 22, 2012

Abstract

The goal of this paper is to generalize the BEM-based FEM for second order elliptic boundary value problems to three space dimensions with the emphasis on polyhedral meshes with polygonal faces, where even non-convex elements are allowed. Due to an implicit definition of the trial functions, the strategy yields conforming approximations and is very flexible with respect to the meshes. Thus, it gets into the line of recent developments in several areas. The arising local problems are treated by two dimensional Galerkin schemes coming from finite and boundary element formulations. With the help of a new interpolation operator and its properties, convergence estimates are proven in the H^1- as well as in the L_2-norm. Numerical experiments confirm the theoretical results.

Keywords BEM-based FEM · polyhedral mesh · convergence estimates · non-standard finite element method

Mathematics Subject Classification (2000) 65N30 · 65N38 · 41A25 · 41A30

1 Introduction

The finite element method (FEM) is a powerful tool for the approximation of solutions of boundary value problems. Its history goes back to the mid of the nineteenth-century. Since that time, there have been a lot of developments for the method which is usually applied on simplicial meshes. Nowadays, the need for more general meshes is arising and thus schemes like finite volume [18], discontinuous Galerkin [10], multiscale finite element [13] or mimetic discretization methods [5] as well as virtual element methods [2] are sometimes favourable over the classic finite element approach. These strategies are applicable on more general meshes due to their nature. But also within the finite element method, there are some developements towards polygonal and polyhedral meshes, see [14, 15, 23]. Such meshes appear naturally in geological and biological science but also while

meshing complex geometries where simplicial elements can be restrictive and deteriorate the mesh quality.
In 2009, D. Copeland, U. Langer and D. Pusch [8] proposed a new strategy which goes back to boundary element domain decomposition methods. This approach uses locally implicit defined trial functions in the finite element method such that it is applicable on general polygonal meshes in two space dimensions. This promising approach, also called BEM-based FEM, has been studied concerning convergence [16, 17], higher order trial functions [21] as well as in an adaptive strategy [24]. Already in [9], the method was formulated in three space dimension on polyhedral meshes and this formulation has been used in the literature cited above. Unfortunately, the polyhedral elements are restricted to those with only triangular faces. The aim of this presentation is to generalize the lowest order trial functions to arbitrary polyhedral elements with polygonal faces. We even relax the convexity of the elements and prove linear convergence in the H^1-norm and quadratic convergence in the L_2-norm with respect to the mesh size.
The article is organized as follows. In Section 2, we state the model problem, give a definition of regular and stable meshes and review the boundary element method (BEM) which is utilized in the numerical realization. The trial functions are introduced in Section 3 and we discuss the set up of the finite element matrix. A priori error estimates are proven in Section 4 and finally, we present numerical experiments in Section 5 which confirm the theoretical results and draw some conclusion.

2 Preliminaries

For the sake of simplicity, we restrict ourselves to a model problem. Let $\Omega \subset \mathbb{R}^3$ be a polyhedral and bounded domain with boundary $\Gamma = \Gamma_D \cup \Gamma_N$ which is split into a Dirichlet and a Neumann part. Furthermore, we assume $|\Gamma_D| > 0$ and there is a given source term $f \in L_2(\Omega)$, a Dirichlet datum $g_D \in H^{1/2}(\Gamma_D)$ as well as a Neumann datum $g_N \in L_2(\Gamma_N)$. We consider the boundary value problem

$$\begin{aligned} -\mathrm{div}(a\nabla u) &= f \quad && \text{in } \Omega, \\ u &= g_D && \text{on } \Gamma_D, \\ a\nabla u \cdot n &= g_N && \text{on } \Gamma_N, \end{aligned} \tag{1}$$

for $a \in L_\infty(\Omega)$ with $0 < a_{\min} \leq a \leq a_{\max}$ on $\overline{\Omega}$. By the use of an extension $u_D \in H^1(\Omega)$ of the Dirichlet datum, the Galerkin formulation for (1) with the solution $u = u_0 + u_D \in H^1(\Omega)$ reads

$$\text{Seek } u_0 \in V: \quad a_\Omega(u_0, v) = \ell(v) \quad \forall v \in V \tag{2}$$

with

$$a_\Omega(u, v) = \int_\Omega a\nabla u \cdot \nabla v$$

and

$$\ell(v) = (f, v)_\Omega + (g_N, v)_{\Gamma_N} - a_\Omega(u_D, v),$$

where

$$V = H^1_D(\Omega) = \left\{ v \in H^1(\Omega) : \gamma_0 v = 0 \text{ on } \Gamma_D \right\}.$$

Here, $\gamma_0 : H^1(\Omega) \to H^{1/2}(\Gamma)$ denotes the usual trace operator, see [1], and $(\cdot,\cdot)_\Omega$ and $(\cdot,\cdot)_{\Gamma_N}$ denote the L_2-scalar products over Ω and Γ_N, respectively. Due to the properties of the material coefficient $a \in L_\infty(\Omega)$ the bilinear form

$$a_\Omega(\cdot,\cdot) : H^1(\Omega) \times H^1(\Omega) \to \mathbb{R}$$

is bounded and coercive on V, i.e. there are constants $m, M > 0$ such that

$$|a_\Omega(u, v)| \leq M \|u\|_{H^1(\Omega)} \|v\|_{H^1(\Omega)} \quad \text{and} \quad a_\Omega(v, v) \geq m \|v\|^2_{H^1(\Omega)},$$

for all $u, v \in V \subset H^1(\Omega)$. Since $\ell(\cdot) : H^1(\Omega) \to \mathbb{R}$ is also bounded on V, the variational formulation (2) admits a unique solution according to the lemma of Lax-Milgram, see [7]. Due to the boundedness and coercivity of the bilinear form, the energy norm $\|\cdot\|_E = \sqrt{a_\Omega(\cdot,\cdot)}$ is equivalent to the usual Sobolev norm $\|\cdot\|_{H^1(\Omega)}$ on V.

The next step in finite element methods is to discretize the domain Ω and to introduce a finite dimensional subspace V_h of V such that we obtain a discrete Galerkin formulation which turns into a system of linear equations. The introduction of V_h and the set up of the system are addressed in Section 3. At this point, we discuss the discretization of the domain. As we have mentioned at the beginning, we allow arbitrary polyhedral meshes with polygonal faces that fulfill some regularity and stability conditions.

A discretization of the domain or also called mesh is denoted by $\mathcal{K}_h$ and it consists of polyhedral elements $K \in \mathcal{K}_h$, polygonal faces $F \in \mathcal{F}_h$, edges $E \in \mathcal{E}_h$ and nodes $z \in \mathcal{N}_h$, where $\mathcal{F}_h$, $\mathcal{E}_h$ and $\mathcal{N}_h$ are the sets of faces, edges and nodes in the mesh. With $\mathcal{N}_{h,D}$, we indicate the nodes which lie on Γ_D or on the transition lines between the Dirichlet and Neumann boundary. The sets of nodes, edges and faces which belong to an element $K \in \mathcal{K}_h$ are labeled $\mathcal{N}(K)$, $\mathcal{E}(K)$ and $\mathcal{F}(K)$, respectively. In the same manner, we define $\mathcal{N}(F)$ and $\mathcal{E}(F)$ for $F \in \mathcal{F}_h$ as the sets of the corresponding nodes and edges. The elements, faces and edges are assumed to be three, two and one dimensional open sets. The diameter of an element $K \in \mathcal{K}_h$, a face $F \in \mathcal{F}_h$ and the length of an edge $E \in \mathcal{E}_h$ are denoted by h_K, h_F and h_E, respectively.

Definition 1. A set of faces $\mathcal{F}_h$ is called regular if all faces are flat and there is a constant $\sigma_\mathcal{F}$ such that every face $F \in \mathcal{F}_h$ is star-shaped with respect to a circle inscribed in F with radius ρ_F and center z_F and the aspect ratio h_F/ρ_F is uniformly bounded from above by $\sigma_\mathcal{F}$ for all $F \in \mathcal{F}_h$.

Definition 2. A mesh $\mathcal{K}_h$ is called regular if the associated set of faces $\mathcal{F}_h$ is regular and if there is a constant $\sigma_{\mathcal{K}}$ such that every element $K \in \mathcal{K}_h$ is star-shaped with respect to a ball inscribed in K with radius ρ_K and center z_K and the aspect ratio h_K/ρ_K is uniformly bounded from above by $\sigma_{\mathcal{K}}$ for all $K \in \mathcal{K}_h$.

Definition 3. A mesh $\mathcal{K}_h$ is called stable if there is a constant $c_{\mathcal{K}}$ such that for every $K \in \mathcal{K}_h$ the estimate $h_K \leq c_{\mathcal{K}} h_E$ for all $E \in \mathcal{E}(K)$ holds true.

In the following, we always consider regular and stable meshes $\mathcal{K}_h$. Note that the elements are star-shaped with respect to a ball and thus non-convex elements are allowed in the discretization. Nevertheless, each element is a Lipschitz domain by itself and we have

$$h_E \leq h_F \leq h_K \leq c_{\mathcal{K}} h_E \leq c_{\mathcal{K}} h_F$$

for $K \in \mathcal{K}_h$ and all $F \in \mathcal{F}(K)$ and $E \in \mathcal{E}(F)$.
An alternative approach to the finite element method is the so called boundary element method. In the case of a constant material parameter $a(\cdot)$ and vanishing right hand side f in (1) we end up with the Laplace equation. We consider this equation on an arbitrary element $K \in \mathcal{K}_h$ and prescribe some Dirichlet data on the boundary, i.e.

$$\begin{aligned} -\Delta u &= 0 \quad \text{in } K, \\ u &= g \quad \text{on } \partial K. \end{aligned} \tag{3}$$

With the help of the so called fundamental solution of minus the Laplacian, which is

$$U^*(x,y) = \frac{1}{4\pi|x-y|} \quad \text{for } x, y \in \mathbb{R}^3,$$

the usual trace operator $\gamma_0^K : H^1(K) \to H^{1/2}(\partial K)$ as well as the conormal derivative, which takes the form

$$\gamma_1^K v = n_K \cdot \gamma_0^K \nabla v \in H^{-1/2}(\partial K)$$

for sufficient regular v and the outer unite normal vector n_K to ∂K, we have the representation formula

$$u(x) = \int_{\partial K} U^*(x,y) \gamma_1^K u(y)\, ds_y - \int_{\partial K} \gamma_{1,y}^K U^*(x,y) \gamma_0^K u(y)\, ds_y \quad \text{for } x \in K. \tag{4}$$

Applying the trace and the conormal derivative operators to this formula, it is possible to derive the relation between the Dirichlet datum $\gamma_0^K u$ and the Neumann datum $\gamma_1^K u$ on ∂K. It is

$$\gamma_1^K u = \mathbf{S}_K \gamma_0^K u \quad \text{with} \quad \mathbf{S}_K = \mathbf{V}_K^{-1} \left(\tfrac{1}{2}\mathbf{I} + \mathbf{K}_K \right), \tag{5}$$

where the operator

$$\mathbf{S}_K : H^{1/2}(\partial K) \to H^{-1/2}(\partial K)$$

is called Steklov-Poincaré operator. Here, we have used the standard boundary integral operators which are well studied, see e.g. [19, 22]. For $x \in \partial K$, we have the single-layer potential operator

$$(\mathbf{V}_K \zeta)(x) = \gamma_0^K \int_{\partial K} U^*(x,y)\zeta(y)\, ds_y \quad \text{for } \zeta \in H^{-1/2}(\partial K)$$

as well as the double-layer potential operator

$$(\mathbf{K}_K \xi)(x) = \lim_{\varepsilon \to 0} \int_{y \in \partial K : |y-x| \geq \varepsilon} \gamma_{1,y}^K U^*(x,y)\xi(y)\, ds_y \quad \text{for } \xi \in H^{1/2}(\partial K).$$

In the numerical realization, these operators have to be approximated. For this reason, a Galerkin scheme is utilized on the boundary ∂K. The first step is to discretize the boundary of K with an admissible triangulation. The boundary mesh is denoted by $\mathcal{B}_h = \mathcal{B}_h(K)$ and its elements, the triangles, by T. The set of nodes is labeled $\mathcal{M}_h = \mathcal{M}_h(K)$. For each $T \in \mathcal{B}_h$, we define a function

$$\tau_T^0 = \begin{cases} 1, & \text{in } T \\ 0, & \text{else} \end{cases} \qquad \text{and set} \qquad \Phi_N = \{\tau_T^0 : T \in \mathcal{B}_h\},$$

which is a basis of the space of piecewise constant functions over the mesh $\mathcal{B}_h$. It is $\operatorname{span} \Phi_N \subset H^{-1/2}(\partial K)$, and thus we use this discrete space for the approximation of the Neumann trace. Additionally, we define for $z \in \mathcal{M}_h$ a function

$$\varphi_z = \begin{cases} 1, & \text{at } z \\ \text{linear}, & \text{on } T \in \mathcal{B}_h \\ 0, & \text{at } x \in \mathcal{M}_h \setminus \{z\} \end{cases} \qquad \text{and set} \qquad \Phi_D = \{\varphi_z : z \in \mathcal{M}_h\}. \tag{6}$$

These functions form a basis of the space of piecewise linear and globally continuous functions over the boundary ∂K. Therefore, it is $\operatorname{span} \Psi_D \subset H^{1/2}(\partial K)$ and we use this discrete space for the approximation of the Dirichlet trace.
In the boundary value problem (3) the Dirichlet datum $g \in H^{1/2}(\partial K)$ is given and we approximate it by $g_h \in \operatorname{span} \Phi_D$. This datum is used in a discrete Galerkin formulation for (5)

$$\text{Seek } t_h \in \operatorname{span} \Phi_N : \quad (\mathbf{V}_K t_h, \vartheta)_{L_2(\partial K)} = \left(\left(\tfrac{1}{2}\mathbf{I} + \mathbf{K}_K \right) g_h, \vartheta \right)_{L_2(\partial K)} \quad \forall \vartheta \in \Phi_N$$

to approximate the unknown Neumann datum $t = \gamma_1^K u \in H^{-1/2}(\partial K)$. Due to the properties of the boundary integral operators, the variational formulation has a unique solution. The representations

$$t_h = \sum_{\tau \in \Phi_N} t_\tau \tau \qquad \text{and} \qquad g_h = \sum_{\varphi \in \Phi_D} g_\varphi \varphi$$

yield the system of linear equations

$$\mathbf{V}_{K,h}\underline{t}_h = \left(\tfrac{1}{2}\mathbf{M}_{K,h} + \mathbf{K}_{K,h}\right)\underline{g}_h,$$

where the underline refers to the coefficient vector, e.g. $\underline{t}_h = (t_\tau)_{\tau\in\Phi_N}$. The matrices are defined as

$$\mathbf{V}_{K,h} = \Big((\mathbf{V}_K\tau, \vartheta)_{L_2(\partial K)}\Big)_{\vartheta\in\Phi_N,\tau\in\Phi_N}$$

and

$$\mathbf{M}_{K,h} = \Big((\varphi, \vartheta)_{L_2(\partial K)}\Big)_{\vartheta\in\Phi_N,\varphi\in\Phi_D}, \quad \mathbf{K}_{K,h} = \Big((\mathbf{K}_K\varphi, \vartheta)_{L_2(\partial K)}\Big)_{\vartheta\in\Phi_N,\varphi\in\Phi_D}.$$

After the computation of $\underline{t}_h$, we use the approximations $g_h \in \operatorname{span}\Phi_D$ of the Dirichlet datum and $t_h \in \operatorname{span}\Phi_N$ of the Neumann datum in the representation formula (4) to obtain an approximation of the exact solution u of (3) in K.

3 BEM-based FEM in 3D

In this section, we discuss the generalization of the BEM-based finite element method studied for the two dimensional case in [21, 24]. So, we address the definition of trial functions on meshes with polyhedral elements which satisfy the regularity of Definition 2. These functions are used to construct an approximation space V_h which can be utilized in the discrete Galerkin formulation of the finite element method. The idea of the BEM-based FEM is to define the trial functions implicitly on each element as local solutions of the underlying differential equation. Here, the coefficients are approximated by piecewise constants and the right hand side is neglected, see [8]. For our model problem, we end up with the Laplace equation.
In order to get a nodal basis of V_h, we declare for each node $z \in \mathcal{N}_h$ a trial function ψ_z which is equal to one in z and zero in all other nodes of the mesh. In [21, 24], the authors used linear data on the edges for the two dimensional case. So more precise, they defined ψ_z as unique solution of

$$\begin{gathered}
-\Delta\psi_z = 0 \quad \text{in } K \quad \text{for all elements } K,\\
\psi_z(x) = \begin{cases} 1 & \text{for } x = z \\ 0 & \text{for all other nodes } x \end{cases},\\
\psi_z \text{ is linear on each edge of } K,
\end{gathered}$$

where the elements K are convex polygons. In the case of polyhedral elements with triangulated surfaces, we can get a straightforward generalization by replacing the word 'edge' by 'triangular face'. This strategy is chosen in the present literature [9, 16, 17].

To handle arbitrary polygonal faces of the polyhedral elements, we follow another strategy. If we look again into the two dimensional case, we observe that the values of the trial functions are fixed in the nodes and extended uniquely along the edges by linear functions. This linear extension is nothing else than an harmonic extension along the edge and thus the trial function is also defined on the edges according to the underlying differential equation. Therefore, we propose a stepwise construction for the trial functions in the case of polyhedral elements with polygonal faces as sketched in Figure 1.

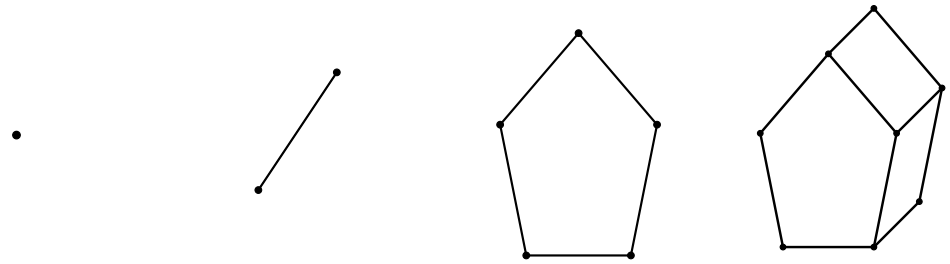

$\psi \in \{0,1\}$ $\quad$ $\Delta_1\psi = \psi'' = 0$ $\quad$ $\Delta_2\psi = 0$ $\quad$ $\Delta_3\psi = 0$

Figure 1: Stepwise construction of trial functions

Denoting the i-dimensional Laplace operator by Δ_i, we define the trial function ψ_z, which belongs to $z \in \mathcal{N}_h$, as unique solution of

$$\begin{aligned} -\Delta_3\psi_z &= 0 \quad \text{in } K \quad \text{for all } K \in \mathcal{K}_h, \\ -\Delta_2\psi_z &= 0 \quad \text{in } F \quad \text{for all } F \in \mathcal{F}_h, \\ -\Delta_1\psi_z &= 0 \quad \text{in } E \quad \text{for all } E \in \mathcal{E}_h, \\ \psi_z(x) &= \begin{cases} 1 & \text{for } x = z \\ 0 & \text{for } x \in \mathcal{N}_h \setminus \{z\} \end{cases}, \end{aligned}$$

where the Laplace operators have to be understood in the corresponding linear parameter spaces. So, the values in the nodes are prescribed. Afterwards, we solve a Dirichlet problem for the Laplace equation on each edge. Then, we use the computed data as Dirichlet datum for the Laplace problem on each face, and finally we proceed with the Laplace problem on each element, where the solutions on the faces are used as boundary values. In the case of convex faces and elements, these problems are understood in the classical sense and we have $\psi_z \in C^2(K) \cap C^0(\overline{K})$. In the more general situation of non-convex elements, the weak solution is considered such that we have at least $\psi_z \in H^1(K)$.

Remark 1. The novel inside into the BEM-based FEM is to define the trial function implicitly on the edges, faces, and elements and not only, as in previous

publications, on the element level. In particular, considering a Helmholtz or convection-diffusion equation, the trial functions already become non-linear on the edges and the properties of the differential equation are build into the trial functions on all levels, on the edges, faces, and elements.

We set

$$\Psi_h = \{\psi_z : z \in \mathcal{N}_h\} \quad \text{as well as} \quad \Psi_D = \{\psi_z : z \in \mathcal{N}_{h,D}\},$$

and we introduce the trial space

$$V_h = \operatorname{span} \Psi \quad \text{with} \quad \Psi = \Psi_h \setminus \Psi_D.$$

According to the regularity of the trial functions inside the elements and their continuity across the element boundaries, the trial space is conforming in the sense of $V_h \subset V$. The discrete version of the Galerkin formulation (2) for the approximation u_h of the exact solution u with $u_h = u_{0h} + u_{Dh}$ and

$$u_{0h} = \sum_{\psi \in \Psi} \beta_\psi \psi \in V_h \quad \text{as well as} \quad u_{Dh} = \sum_{\psi \in \Psi_D} \beta_\psi \psi$$

reads

$$\sum_{\psi \in \Psi} \beta_\psi \, a_\Omega(\psi, \phi) = (f, \phi)_\Omega + (g_N, \phi)_{\Gamma_N} - \sum_{\psi \in \Psi_D} \beta_\psi \, a_\Omega(\psi, \phi) \quad \text{for } \phi \in \Psi,$$

where u_{Dh} is the discrete extension of the boundary data g_D in the model problem (1). In the representations of u_{0h} and u_{Dh} the same symbol β_ψ is used for the coefficients, but there should be no confusion since $\Psi \cap \Psi_D = \varnothing$.
If there are only triangular faces of the polyhedra, the definition of the trial space agrees with the former generalization. Otherwise, we have to solve additional Dirichlet boundary value problems on the faces of the elements. This can be done by the help of a two dimensional boundary element method. Nevertheless, we propose to use a 2D finite element method on triangular meshes of the faces. For each $F \in \mathcal{F}_h$, we introduce a mesh $\mathcal{B}_h(F)$ of level l. The coarsest mesh with $l = 0$ is obtained by connecting the nodes $z \in \mathcal{N}(F)$ with the point z_F, which is fixed once per face according to Definition 1. Afterwards, the meshes of level $l \geq 1$ are defined recursively by splitting each triangle of the previous level into four similar triangles. So, the midpoints of the sides of a triangle are connected successively, see Figure 2. The set of nodes in the triangular mesh is denoted by $\mathcal{M}_h(F)$. Obviously, we can combine the discretizations of the faces to a triangulation of the whole surface of an element $K \in \mathcal{K}_h$ by setting

$$\mathcal{B}_h(K) = \bigcup_{F \in \mathcal{F}(K)} \mathcal{B}_h(F) \quad \text{and} \quad \mathcal{M}_h(K) = \bigcup_{F \in \mathcal{F}(K)} \mathcal{M}_h(F).$$

Due to the construction, the surface mesh $\mathcal{B}_h(K)$ is conforming. Now, we address the approximation of the trace of a trial function ψ_z, $z \in \mathcal{N}_h$ on a face $F \in \mathcal{F}_h$

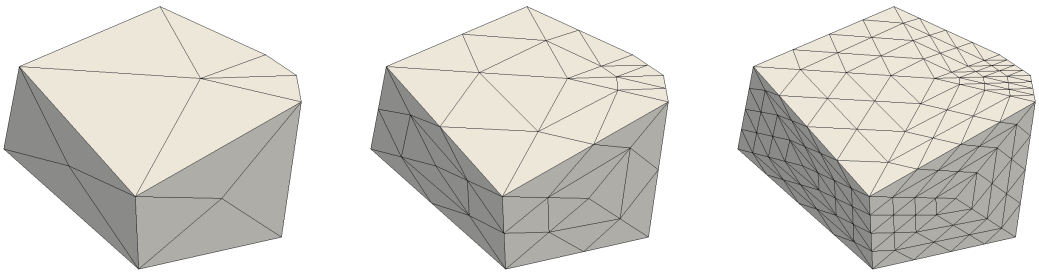

Figure 2: Polyhedral element with surface triangulations of level $l = 0, 1, 2$

with $z \in \mathcal{N}(F)$. For the finite element computations on the face, we have to use a further trial space. Here, we utilize the usual basis $\Phi_D(F)$ of piecewise linear and continuous functions. It is

$$\Phi_D(F) = \{\varphi_z : z \in \mathcal{M}_h(F)\},$$

compare (6). We approximate the trace of the trial function ψ_z by

$$g_z^F = \sum_{\varphi \in \Phi_D(F)} g_\varphi \varphi,$$

where the coefficients g_φ which belong to $\varphi = \varphi_x$ with $x \in \partial F$ are fixed such that g_z^F coincides with the piecewise linear data of ψ_z on the edges of the face F. Consequently, we obtain the discrete Galerkin formulation

$$\text{Seek } g_z^F : \quad \sum_{x \in \mathcal{M}_h(F)} g_{\varphi_x} \int_F \nabla \varphi_x \cdot \nabla \varphi_y = 0, \quad \forall y \in \mathcal{M}_h(F) : y \notin \partial F,$$

for the approximation of the trace of ψ_z on $F \in \mathcal{F}_h$, where $z \in \mathcal{N}(F)$. This discrete variational formulation admits a unique solution and the corresponding system of linear equations can be solved by a conjugate gradient method, for example. Changing the level of the face discretization, the accuracy of the finite element approximation can be adapted.

Remark 2. In the case of another differential equation like for Helmholtz or convection-diffusion problems, we should choose a mesh level $l \geq 1$ for the faces. This automatically implies a discretization of the edges which can be used to handle the non-linear data of the trial functions along the edges in the 2D finite element method on the faces.

To get an approximation g_z^K of the trace of ψ_z on the whole boundary of an element $K \in \mathcal{K}_h$, the Dirichlet problems on the faces $F \in \mathcal{F}(K)$ are solved successively. Afterwards, these approximations are combined to

$$g_z^K = \sum_{\varphi \in \Phi_D(K)} g_\varphi \varphi \quad \text{with} \quad \Phi_D(K) = \bigcup_{F \in \mathcal{F}(K)} \Phi_D(F).$$

Thus, we obtain a piecewise linear and globally continuous approximation of the Dirichlet trace $\gamma_0^K \psi_z$ over the surface triangulation $\mathcal{B}_h(K)$. In the numerics, we use this approximated datum instead of the exact boundary values of the trial functions to define ψ_z. Therefore, we only obtain approximations of the introduced trial functions and we rather work with an approximated space V_l of V_h than with V_h directly. Let us define

$$\Psi_l = \{\psi_z^l : z \in \mathcal{N}_h\} \quad \text{as well as} \quad \Psi_{D,l} = \{\psi_z^l : z \in \mathcal{N}_{h,D}\},$$

where ψ_z^l is the unique solution of

$$\begin{aligned} -\Delta \psi_z^l &= 0 \quad && \text{in } K, \\ \psi_z^l &= g_z^K && \text{on } \partial K \end{aligned}$$

for all $K \in \mathcal{K}_h$. Additionally, we set

$$V_l = \operatorname{span} \Psi \quad \text{with} \quad \Psi = \Psi_l \setminus \Psi_{D,l}$$

and obtain another conforming approximation space $V_l \subset V$ which depends on the auxiliary triangulations of the faces and especially on their discretization level l. The trial function ψ_z^l approximates the function ψ_z. If it is clear from the context which function is meant and the level is not important, we skeep the index l in the following.
In the computational realization, we actually solve the discrete Galerkin method which is obtained by exchanging V_h, Ψ_h and Ψ_D by V_l, Ψ_l and $\Psi_{D,l}$ in the discrete variational formulation above. That means, we seek an approximation u_l of the exact solution u with $u_l = u_{0l} + u_{Dl}$ and

$$u_{0l} = \sum_{\psi \in \Psi} \beta_\psi \psi \in V_l \quad \text{as well as} \quad u_{Dl} = \sum_{\psi \in \Psi_{D,l}} \beta_\psi \psi \tag{7}$$

fulfilling

$$\sum_{\psi \in \Psi} \beta_\psi \, a_\Omega(\psi, \phi) = (f, \phi)_\Omega + (g_N, \phi)_{\Gamma_N} - \sum_{\psi \in \Psi_{D,l}} \beta_\psi \, a_\Omega(\psi, \phi) \quad \text{for } \phi \in \Psi, \tag{8}$$

where u_{Dl} is a discrete extension of the boundary data g_D and $\Psi = \Psi_l \setminus \Psi_{D,l}$.
The next task is to discuss the approximation of the several terms in the discrete Galerkin formulation. The L_2-scalar product over the Neuman boundary is rather simple. The trial functions are given as piecewise linear on a triangulation of Γ_N. Therefore, a standard Gaussian quadrature can be used on each triangle. To handle the L_2-scalar product over Ω, we use a quadrature over polyhedral elements. This can be done by refining the element into tetrahedra or by using directly a numerical integration scheme for polyhedral domains, see [20]. The evaluations

of the trial functions are realized with the help of boundary element methods. Thus, the Neumann traces of the trial functions have to be approximated.
At this point, it becomes clear why we have chosen a finite element discretization of the faces. The surface mesh $\mathcal{B}_h(K)$ and the trial functions on the boundary ∂K for the two dimensional finite element method fit into the theory of the boundary element method reviewed in Section 2. Following the ideas given there, we obtain an approximation t_z^K of the Neumann trace $\gamma_1^K \psi_z$ in the form

$$t_z^K = \sum_{\tau \in \Phi_N(K)} t_\tau \tau \qquad \text{with} \qquad \underline{t}_z^K = \mathbf{V}_{K,h}^{-1}(\tfrac{1}{2}\mathbf{M}_{K,h} + \mathbf{K}_{K,h})\underline{g}_z^K. \tag{9}$$

For each element $K \in \mathcal{K}_h$, the approximations of the Dirichlet and Neumann traces of the trial functions ψ_z with $z \in \mathcal{N}(K)$ are gathered in the matrices

$$D_K = \left(\underline{g}_z^K \right)_{z \in \mathcal{N}(K)} \qquad \text{and} \qquad N_K = \left(\underline{t}_z^K \right)_{z \in \mathcal{N}(K)}$$

such that each column corresponds to the datum of one ψ_z. The relation (9) turns into

$$N_K = \mathbf{V}_{K,h}^{-1}(\tfrac{1}{2}\mathbf{M}_{K,h} + \mathbf{K}_{K,h})D_K.$$

For a better understanding, we give the dimensions of the matrices

$$\begin{aligned} \mathbf{V}_{K,h} &\in \mathbb{R}^{|\mathcal{B}_h(K)| \times |\mathcal{B}_h(K)|} & D_K &\in \mathbb{R}^{|\mathcal{M}_h(K)| \times |\mathcal{N}(K)|} \\ \mathbf{K}_{K,h} &\in \mathbb{R}^{|\mathcal{B}_h(K)| \times |\mathcal{M}_h(K)|} & N_K &\in \mathbb{R}^{|\mathcal{B}_h(K)| \times |\mathcal{N}(K)|} \\ \mathbf{M}_{K,h} &\in \mathbb{R}^{|\mathcal{B}_h(K)| \times |\mathcal{M}_h(K)|}. \end{aligned} \tag{10}$$

In the global finite element computation, the number of degrees of freedom which correspond to the element K is $|\mathcal{N}(K)|$. For the local computations, we use $|\mathcal{B}_h(K)|$ degrees of freedom to approximate the Neumann trace of each trial function and the Dirichlet trace is represented by $|\mathcal{M}_h(K)|$ coefficients. Obviously, we have

$$|\mathcal{N}(K)| \leq |\mathcal{M}_h(K)| \qquad \text{and} \qquad |\mathcal{F}(K)| \leq |\mathcal{B}_h(K)|.$$

Since we know how to approximate the Dirichlet and Neumann data of the trial functions on the element boundaries, we can use the representation formula (4) to get an approximation inside the elements.
Finally, we consider the approximation of the bilinear form $a_\Omega(\cdot, \cdot)$. We assume that the material coefficient is constant on each element such that

$$a(x) = a_K \quad \text{for } x \in K \text{ and } K \in \mathcal{K}_h,$$

or it is approximated by a piecewise constant function. Let $\psi, \phi \in \Psi$, it is

$$a_\Omega(\psi, \phi) = \sum_{K \in \mathcal{K}_h} a_K \int_K \nabla\psi \cdot \nabla\phi = \sum_{K \in \mathcal{K}_h} \frac{a_K}{2} \left(\int_{\partial K} \gamma_1^K \psi \gamma_0^K \phi + \int_{\partial K} \gamma_1^K \phi \gamma_0^K \psi \right)$$

according to Green's first identity and since ψ as well as ϕ are harmonic on each element $K \in \mathcal{K}_h$. Obviously, there are $x, z \in \mathcal{N}_h$ such that $\psi = \psi_x$ and $\phi = \psi_z$ and if there is no $K \in \mathcal{K}_h$ with $x, z \in \mathcal{N}(K)$, we have $a_\Omega(\psi, \phi) = 0$. On the other hand, for each $K \in \mathcal{K}_h$ with $x, z \in \mathcal{N}(K)$ we get the approximations g_x^K, g_z^K for the Dirichlet traces and t_x^K, t_z^K for the Neumann traces of the trial functions ψ_x and ψ_z out of the matrices D_K and N_K, respectively. For the integrals in the representation of the bilinear form above, we choose the approximation

$$\int_{\partial K} \gamma_1^K \psi_x \gamma_0^K \psi_z \approx \int_{\partial K} t_x^K g_z^K = \sum_{\tau \in \Phi_N(K)} t_\tau \sum_{\varphi \in \Phi_D(K)} g_\varphi(\tau, \varphi)_{L_2(\partial K)} = \left(\underline{t}_x^K\right)^\top \mathbf{M}_{K,h}\, \underline{g}_z^K$$

with the mass matrix $\mathbf{M}_{K,h}$ defined as in Section 2. This yields the symmetric approximation

$$a_\Omega(\psi_x, \psi_z) \approx \sum_{K \in \mathcal{K}_h} \frac{a_K}{2} \left(\left(\underline{t}_x^K\right)^\top \mathbf{M}_{K,h}\, \underline{g}_z^K + \left(\underline{t}_z^K\right)^\top \mathbf{M}_{K,h}\, \underline{g}_x^K \right), \tag{11}$$

where the coefficient vectors are identical to zero if $x \notin \mathcal{N}(K)$ and $z \notin \mathcal{N}(K)$, respectively. Consequently, we use the local matrix

$$N_K^\top\, \mathbf{M}_{K,h}\, D_K \in \mathbb{R}^{|\mathcal{N}(K)| \times |\mathcal{N}(K)|}$$

for each $K \in \mathcal{K}_h$ to set up the global finite element matrix. Due to the symmetric approximation (11) of the bilinear form, we obtain a symmetric system matrix in the finite element method which is sparse and positive definite. Therefore, the conjugate gradient method is applied to get the solution of the system of linear equations.

Remark 3. Before the finite element matrix is set up, it is necessary to compute the approximations of the Dirichlet problems on the faces and to get the Neumann traces. This is done in a preprocessing step where first the 2D finite element approximations on the faces and afterwards the boundary integral matrices as well as the Neumann traces are computed. Each step is fully parallelizable since the problems on the faces as well as those on the elements are independent from each other.

4 Convergence estimates

Let $u = u_0 + u_D$ be the solution of the model problem obtained by the variational formulation (2) and $u_l = u_{0l} + u_{Dl}$ its Galerkin approximation gained by (7) and (8) with the approximated trial space V_l. We assume that the extension of the Dirichlet datum g_D can be chosen such that $u_D = u_{Dl} \in \operatorname{span} \Psi_l$. In this section, our goal is to introduce an interpolation operator $\mathfrak{I}_l : H^2(\Omega) \to \operatorname{span} \Psi_l$ such that

$$\|v - \mathfrak{I}_l v\|_{H^1(\Omega)} \leq ch\, |v|_{H^2(\Omega)} \quad \text{for } v \in H^2(\Omega), \tag{12}$$

where $h = \max\{h_K : K \in \mathcal{K}_h\}$. The definition of an interpolation operator with this approximation property is a non-trivial task. However, it is an important tool for theoretical considerations and it enables us to prove the following convergence estimates.

Theorem 1. *Let $\mathcal{K}_h$ be a regular and stable mesh of a bounded polyhedral domain $\Omega \subset \mathbb{R}^3$. Then, it is*

$$\|u - u_l\|_{H^1(\Omega)} \leq ch\,|u|_{H^2(\Omega)} \quad \textit{for } u \in H^2(\Omega),$$

where the constant c only depends on the regularity and stability parameters of the mesh and on the level l.

Proof. Since $V_l \subset V$ is a conforming approximation space, we can apply Céa's lemma, see [7], which yields

$$\|u - u_l\|_{H^1(\Omega)} \leq \frac{M}{m} \min_{v \in u_{Dl} + V_l} \|u - v\|_{H^1(\Omega)} \leq \frac{M}{m} \|u - \mathfrak{I}_l u\|_{H^1(\Omega)},$$

where we used $\mathfrak{I}_l u \in u_{Dl} + V_l$ with the notation

$$u_{Dl} + V_l = \{v_l + u_{Dl} : v_l \in V_l\} \subset \operatorname{span} \Psi_l.$$

The property (12) of the interpolation operator finishes the proof. □

Remark 4. For the estimate in the theorem, we have implicitly assumed that there are no errors in the evaluation of the bilinear form and the right hand side of the Galerkin formulation. The case of approximate data f, g_D, g_N in the discrete problem can be treated in the usual way, where the Strang lemma is used instead of Céa's lemma, see [7].

The change of the norm in which the finite element error is measured gives an additional power of h if the adjoint variational formulation admits a sufficiently regular solution.

Theorem 2. *Let $\mathcal{K}_h$ be a regular mesh of a bounded polyhedral domain $\Omega \subset \mathbb{R}^3$. Under the condition that for any $g \in L_2(\Omega)$ there is a unique solution of*

$$\textit{Seek } w \in V: \quad a_\Omega(v, w) = (g, v)_\Omega, \quad \forall v \in V,$$

with $w \in H^2(\Omega)$ such that

$$|w|_{H^2(\Omega)} \leq C\,\|g\|_{L_2(\Omega)},$$

it is

$$\|u - u_l\|_{L_2(\Omega)} \leq ch^2\,|u|_{H^2(\Omega)} \quad \textit{for } u \in H^2(\Omega),$$

where the constant c only depends on the regularity and stability parameters of the mesh and on the level l.

Proof. We use the usual Aubin-Nitsche trick, see [7]. Since $u - u_l \in V \subset L_2(\Omega)$ and due to the preliminaries of the theorem, there is a unique function $w \in H^2(\Omega)$ such that

$$a_\Omega(v, w) = (u - u_l, v)_\Omega \quad \text{for } v \in V$$

and

$$|w|_{H^2(\Omega)} \leq C \, \|u - u_l\|_{L_2(\Omega)}.$$

The Galerkin orthogonality

$$a_\Omega(u - u_l, v_l) = 0 \quad \text{for } v_l \in V_l$$

and the continuity of the bilinear form yield for arbitrary $v_l \in V_l$

$$\begin{aligned} \|u - u_l\|^2_{L_2(\Omega)} &= (u - u_l, u - u_l)_\Omega = a_\Omega(u - u_l, w) \\ &= a_\Omega(u - u_l, w - v_l) \leq M \, \|u - u_l\|_{H^1(\Omega)} \|w - v_l\|_{H^1(\Omega)}. \end{aligned}$$

The two terms on the right hand side are estimated separately. For the second one, we choose $v_l = \mathfrak{I}_l w \in V_l$ and obtain with (12)

$$\|w - \mathfrak{I}_l w\|_{H^1(\Omega)} \leq ch|w|_{H^2(\Omega)} \leq ch\|u - u_l\|_{L_2(\Omega)}.$$

The first term $\|u - u_l\|_{H^1(\Omega)}$, which is the approximation error of the finite element method in the H^1-norm, is treated by Theorem 1. Finally, we obtain

$$\|u - u_l\|^2_{L_2(\Omega)} \leq cMh^2 \, |u|_{H^2(\Omega)} \|u - u_l\|_{L_2(\Omega)}.$$

Dividing by $\|u - u_l\|_{L_2(\Omega)}$ yields the desired estimate. □

The rest of this section is devoted to give an appropriate interpolation operator. Since $H^2(\Omega) \subset C^0(\overline{\Omega})$ according to the Sobolev embedding theorem, see [6], the pointwise evaluation of a function $v \in H^2(\Omega)$ is well defined and we can utilize a nodal interpolation operator. We set

$$\mathfrak{I}_l v = \sum_{\psi \in \Psi_l} \alpha_\psi \psi \qquad \text{with} \qquad \alpha_{\psi_z} = v(z) \quad \text{for } z \in \mathcal{N}_h.$$

As in [21], we start studying the properties of the interpolation operator over one element $K \in \mathcal{K}_h$. Consequently, we are just interested in the linear combination of trial functions which belong to nodes in $\mathcal{N}(K)$.

Lemma 1. *The restriction of the interpolation operator $\mathfrak{I}_l$ to an element $K \in \mathcal{K}_h$ fulfills $\mathfrak{I}_l p = p$ on K for each linear polynomial $p \in \mathcal{P}^1(K)$.*

Proof. Let $p \in \mathcal{P}^1(K)$. Obviously, the restriction of p to each face $F \in \mathcal{F}(K)$ and all the edges $E \in \mathcal{E}(F)$ is linear. Due to the definition of the trial functions $\psi^l_z \in \Psi_l$ for $z \in \mathcal{N}(F)$ and the nodal interpolation, p and $\mathfrak{I}_l p$ coincide on the

polygonal boundary ∂F of the face F and both fulfill the weak formulation of the two dimensional Laplace equation in the parameter space of the face $F \in \mathcal{F}(K)$. Since the Galerkin formulation for the Dirichlet problem of the Laplace equation admits a unique solution, the linear function p and its interpolation $\mathfrak{I}_l p$ coincide on all faces $F \in \mathcal{F}(K)$. With the same argument, we obtain $\mathfrak{I}_l p = p$ in K since p and $\mathfrak{I}_l p$ agree on ∂K and fulfill the Laplace equation in K. □

The proof of the next lemma makes use of an auxiliary discretization of the element into tetrahedra. For this reason, we connect all nodes in the triangulation $\mathcal{B}_h(K)$ of ∂K with the center z_K from Definition 2. Such a constructed tetrahedra is denoted by T_{tet} in the following.

Proposition 1. *The auxiliary discretization of an element into tetrahedra, as described above, is regular in the classical sense of finite element methods. So, neighbouring tetrahedra either share a common node, edge or triangular face and the aspect ratio of their diameter $h_{T_{\text{tet}}}$ and the radius $\rho_{T_{\text{tet}}}$ of their insphere is bounded uniformly from above, i.e. $h_{T_{\text{tet}}}/\rho_{T_{\text{tet}}} < \sigma_{\text{tet}}$. Here, σ_{tet} only depends on the regularity and stability parameters of Definitions 2 and 3 and on the level l in the face discretization.*

Proof. For an arbitrary tetrahedron, we have the relation

$$\rho_{\text{tet}} = \frac{3V_{\text{tet}}}{A_{\text{tet}}},$$

where V_{tet} is the volume and A_{tet} is the surface area of the tetrahedron. This relation is seen as follows. The insphere is perpendicular to the faces of the tetrahedron and thus V_{tet} is equal to the sum of the volumes $V_{\text{tet},i}$, $i = 1, \dots, 4$, of the four tetrahedrons obtained by connecting the vertexes with the center of the insphere. Each volume is computed as $V_{\text{tet},i} = \frac{1}{3}\rho_{\text{tet}}|T_i|$, where T_i is the triangle on the surface of the initial tetrahedron. Consequently, it is

$$V_{\text{tet}} = \sum_{i=1}^{4} V_{\text{tet},i} = \sum_{i=1}^{4} \frac{1}{3}\rho_{\text{tet}}|T_i| = \frac{1}{3}\rho_{\text{tet}} A_{\text{tet}}.$$

Let $K \in \mathcal{K}_h$ be an element of a regular and stable mesh. First, we study the case $l = 0$, where only one node per face is added for the triangulation of the element surface. We consider the auxiliary discretization and choose an arbitrary tetrahedron T_{tet} with corresponding triangle $T \in \mathcal{B}_h(F)$ in some face $F \in \mathcal{F}(K)$ and with an edge $E \in \mathcal{E}(F)$ such that $E \subset \partial T \cap \partial F$. A rough estimate for the surface area of this tetrahedron is

$$A_{\text{tet}} = \sum_{i=1}^{4} |T_i| \leq \sum_{i=1}^{4} \frac{h_K^2}{2} = 2h_K^2.$$

Let $\operatorname{dist}(z_K, T)$ be the distance of the center z_K to the triangle T and let h_{TE} be the hight of the triangle T over the edge E. For the volume of T_{tet}, we have

$$V_{\text{tet}} = \frac{1}{3}\operatorname{dist}(z_K, T)|T| = \frac{1}{6}\operatorname{dist}(z_K, T)h_{TE}h_E.$$

Since the faces of the element K and the element itself are star-shaped with respect to circles and a ball according to Definitions 1 and 2, it is $\rho_F \leq h_{TE}$ as well as $\rho_K \leq \operatorname{dist}(z_K, T)$. Consequently, we obtain

$$V_{\text{tet}} \geq \frac{1}{6}\rho_K\rho_F h_E \geq \frac{1}{6\sigma_{\mathcal{K}}\sigma_{\mathcal{F}}}h_K h_F h_E \geq \frac{1}{6\sigma_{\mathcal{K}}\sigma_{\mathcal{F}}}h_E^3.$$

This yields together with the stability in Definition 3

$$\frac{h_{T_{\text{tet}}}}{\rho_{T_{\text{tet}}}} = \frac{h_{T_{\text{tet}}}A_{\text{tet}}}{3V_{\text{tet}}} \leq \frac{4\sigma_{\mathcal{K}}\sigma_{\mathcal{F}}h_K^3}{h_E^3} \leq 4\sigma_{\mathcal{K}}\sigma_{\mathcal{F}}c_{\mathcal{K}}^3.$$

In the case $l \geq 1$, the volume V_{tet} gets smaller. The triangle $T \subset F \in \mathcal{F}(K)$ is obtained by successive splitting of an initial triangle T_0 of the mesh with level zero. Due to the construction, these triangles are similar and the relation $|T| = |T_0|/4^l$ holds. Taking into account this relation in the considerations above gives the general estimate

$$\frac{h_{T_{\text{tet}}}}{\rho_{T_{\text{tet}}}} \leq \sigma_{\text{tet}} \quad \text{with} \quad \sigma_{\text{tet}} = 4^{l+1}\sigma_{\mathcal{K}}\sigma_{\mathcal{F}}c_{\mathcal{K}}^3.$$

□

Lemma 2. *Let $\mathcal{K}_h$ be a regular and stable mesh and $K \in \mathcal{K}_h$ with $h_K = 1$. There exists a constant c which only depends on the regularity and stability parameters as well as on the level l such that*

$$\|\mathfrak{I}_l v\|_{H^1(K)} \leq c\,\|v\|_{H^2(K)} \quad \textit{for } v \in H^2(K).$$

Proof. Let $v \in H^2(K)$. The interpolation $\mathfrak{I}_l v$ fulfills the weak formulation

$$\text{Find } \widetilde{v} \in H^1(K): \quad \gamma_0^K\widetilde{v} = g_v \quad \text{and} \quad (\nabla\widetilde{v}, \nabla w)_{L_2(K)} = 0, \quad \forall w \in H_0^1(K)$$

with a piecewise linear function $g_v = \mathfrak{I}_l v\big|_{\partial K}$ on the boundary. To obtain homogeneous boundary data, we decompose $\widetilde{v} = \widetilde{v}_0 + \widetilde{v}_g$, where $\widetilde{v}_0 \in H_0^1(K)$ and $\widetilde{v}_g \in H^1(K)$ with $\gamma_0^K\widetilde{v}_g = g_v$. According to Proposition 1, the auxiliary discretization of K into tetrahedra is regular in the classical sense of finite elements methods. Therefore, we can use the standard interpolation operator on tetrahedral meshes for linear trial functions to get some $\widetilde{v}_g$. Due to this choice and since $h_K = 1$, it is

$$\|v - \widetilde{v}_g\|_{H^1(K)} \leq C_1\,|v|_{H^2(K)},$$

see [7], where the constant C_1 only depends on the maximal aspect ratio σ_{tet}. The reverse triangular inequality yields

$$\|\widetilde{v}_g\|_{H^1(K)} \leq C_1 \, |v|_{H^2(K)} + \|v\|_{H^1(K)} \leq \max\{1, C_1\} \, \|v\|_{H^2(K)}.$$

The function $\widetilde{v}_0$ fulfills

$$\text{Find } \widetilde{v}_0 \in H^1_0(K): \quad (\nabla \widetilde{v}_0 \cdot \nabla w)_{L_2(K)} = -(\nabla \widetilde{v}_g \cdot \nabla w)_{L_2(K)}, \quad \forall w \in H^1_0(K).$$

Since K can be embedded into a cube with side length h_K, the Poincaré inequality in [3] takes the form

$$\|w\|_{L_2(K)} \leq h_K |w|_{H^1(K)} \quad \text{for } w \in H^1_0(K).$$

According to this inequality and since $h_K = 1$, it is

$$\|\widetilde{v}_0\|^2_{H^1(K)} = \|\widetilde{v}_0\|^2_{L_2(K)} + |\widetilde{v}_0|^2_{H^1(K)} \leq 2|\widetilde{v}_0|^2_{H^1(K)}.$$

Due to the variational formulation for $\widetilde{v}_0$, we find with the help of the Cauchy-Schwarz inequality that

$$|\widetilde{v}_0|^2_{H^1(K)} = \left|(\nabla \widetilde{v}_g, \nabla \widetilde{v}_0)_{L_2(K)}\right| \leq |\widetilde{v}_g|_{H^1(K)} |\widetilde{v}_0|_{H^1(K)}$$

which yields

$$|\widetilde{v}_0|_{H^1(K)} \leq \|\widetilde{v}_g\|_{H^1(K)}.$$

The final step in the proof is to combine all estimates as follows

$$\begin{aligned} \|\mathfrak{I}_l v\|_{H^1(K)} &\leq \|\widetilde{v}_0\|_{H^1(K)} + \|\widetilde{v}_g\|_{H^1(K)} \\ &\leq \sqrt{2} \, |\widetilde{v}_0|_{H^1(K)} + \|\widetilde{v}_g\|_{H^1(K)} \\ &\leq \left(1 + \sqrt{2}\right) \|\widetilde{v}_g\|_{H^1(K)} \\ &\leq \max\{1, C_1\} \left(1 + \sqrt{2}\right) \|v\|_{H^2(K)}. \end{aligned}$$

□

Applying all previous considerations, we are able to prove the interpolation error estimate (12).

Theorem 3. *For a regular and stable mesh $\mathcal{K}_h$ of a bounded polyhedral domain $\Omega \subset \mathbb{R}^3$, the interpolation operators $\mathfrak{I}_l : H^2(\Omega) \to \operatorname{span} \Psi_l$ fulfills*

$$\|v - \mathfrak{I}_l v\|_{H^1(\Omega)} \leq ch \, |v|_{H^2(\Omega)} \quad \textit{for } v \in H^2(\Omega)$$

where $h = \max\{h_K : K \in \mathcal{K}_h\}$ and the constant c only depends on the regularity and stability parameters of the mesh and on the level l.

Proof. Let us start to examine the error over one element $K \in \mathcal{K}_h$. We scale this element such that its diameter becomes one. For this, the transformation $\widehat{x} \mapsto x = z_K + h_K \widehat{x} \in K$ is applied and the scaled element is denoted by $\widehat{K}$. With the notation $\widehat{v}(\widehat{x}) = v(z_K + h_K \widehat{x})$ and the variable transformation in the integrals of the norms, we obtain for $v \in H^2(K)$

$$\begin{aligned} \|v\|_{L_2(K)} &= h_K^{3/2} \|\widehat{v}\|_{L_2(\widehat{K})}, \\ |v|_{H^1(K)} &= h_K^{1/2} |\widehat{v}|_{H^1(\widehat{K})}, \\ |v|_{H^2(K)} &= h_K^{-1/2} |\widehat{v}|_{H^2(\widehat{K})} \end{aligned}$$

and thus $\widehat{v} \in H^2(\widehat{K})$.
Let $\widehat{\mathfrak{I}}_l$ be the interpolation operator with respect to $\widehat{K}$. Due to the pointwise interpolation, it does not matter if v is first transformed into $\widehat{v}$ and then interpolated or vice versa, i.e.

$$\widehat{\mathfrak{I}}_l \widehat{v} = \widehat{\mathfrak{I}_l v}.$$

Consequently, we obtain

$$\begin{aligned} \|v - \mathfrak{I}_l v\|^2_{H^1(K)} &= \|v - \mathfrak{I}_l v\|^2_{L_2(K)} + |v - \mathfrak{I}_l v|^2_{H^1(K)} \\ &= h_K^3 \|\widehat{v} - \widehat{\mathfrak{I}}_l \widehat{v}\|^2_{L_2(\widehat{K})} + h_K |\widehat{v} - \widehat{\mathfrak{I}}_l \widehat{v}|^2_{H^1(\widehat{K})} \\ &\leq h_K \|\widehat{v} - \widehat{\mathfrak{I}}_l \widehat{v}\|^2_{H^1(\widehat{K})} \end{aligned}$$

since $h_K \leq 1$. According to the general approximation theory in Sobolev spaces, see [4], there is a linear polynomial $\widehat{p} \in \mathcal{P}^1(\widehat{K})$ which satisfies

$$|\widehat{v} - \widehat{p}|_{H^k(\widehat{K})} \leq C(k, \sigma_{\mathcal{K}}) |\widehat{v}|_{H^2(\widehat{K})} \quad \text{for } k = 0, 1. \tag{13}$$

Due to the scaling, the constant $C(k, \sigma_{\mathcal{K}})$ is independent on the mesh size h_K. Applying Lemmata 1 and 2, we obtain

$$\begin{aligned} \|\widehat{v} - \widehat{\mathfrak{I}}_l \widehat{v}\|_{H^1(\widehat{K})} &\leq \|\widehat{v} - \widehat{p}\|_{H^1(\widehat{K})} + \|\widehat{\mathfrak{I}}_l (\widehat{v} - \widehat{p})\|_{H^1(\widehat{K})} \\ &\leq (1 + c) \|\widehat{v} - \widehat{p}\|_{H^2(\widehat{K})} \\ &\leq (1 + c) C(\sigma_{\mathcal{K}}) |\widehat{v}|_{H^2(\widehat{K})}, \end{aligned} \tag{14}$$

where we also have used (13) and the fact that the second derivatives of $\widehat{p}$ vanish. Comparing the last two estimates and transforming back to the element K yields

$$\|v - \mathfrak{I}_l v\|^2_{H^1(K)} \leq c h_K |\widehat{v}|^2_{H^2(\widehat{K})} = c h_K^2 |v|^2_{H^2(K)}$$

In the last step of the proof, we have to sum up this inequality over all elements of the mesh and apply the square root to it. This gives

$$\|v - \mathfrak{I}_l v\|_{H^1(\Omega)} \leq c \left(\sum_{K \in \mathcal{K}_h} h_K^2 |v|^2_{H^2(K)} \right)^{1/2} \leq c h |v|_{H^2(K)}$$

and finishes the proof. □

5 Numerical experiments

All numerical examples in this section are formulated on the unite cube. As discretization, we utilize Voronoi meshes which are an example of polyhedral meshes. In Figure 3, the first meshes of the sequence for the convergence experiments are visualized. We see that the elements are non-trivial polyhedra with arbitrary polygonal faces. The meshes have been produced by generating random points according to [12] and constructing the corresponding Voronoi diagram in accordance with [11]. In the set up of the local boundary element matrices, we use a semi analytical integration scheme. The inner integral in the Galerkin matrices is evaluated analytically and the outer one is approximated by Gaussian quadrature.

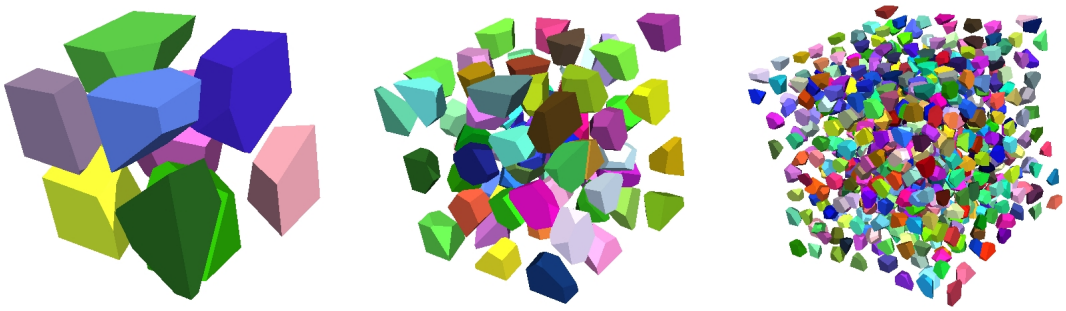

Figure 3: Sequence of Voronoi meshes

In Table 1, we sketch the number of elements $|\mathcal{K}_h|$ and the number of nodes $|\mathcal{N}_h|$ in the different Voronoi meshes. The proposed strategy approximates the solution by a linear combination of as many trial function as nodes are in the mesh. Therefore, the number of degrees of freedom in the finite element method is $|\mathcal{N}_h|$ minus the number of nodes on the Dirichlet boundary Γ_D. The method proposed in [8] needs to triangulate the surfaces of the elements and the number of trial functions corresponds to the total number of nodes after the triangulation. In Table 1, this total number of nodes is listed in the case that the faces are triangulated with

$\lvert\mathcal{K}_h\rvert$	$\lvert\mathcal{N}_h\rvert$	$l=0$	$l=1$	$l=2$
9	46	98	424	1790
76	416	905	4170	18011
712	4186	9081	42446	184170
1316	7850	17013	79676	345903
5606	34427	74457	349663	1519143
26362	164915	356189	1675171	7280603

Table 1: Total number of nodes when working with triangulated surfaces of different mesh levels l

$\lvert\mathcal{N}(K)\rvert$	l	$\lvert\mathcal{M}_h(K)\rvert$	$\lvert\mathcal{B}_h(K)\rvert$
12	0	20	36
	1	74	144
	2	290	576
	3	1154	2304
	4	4610	9216

Table 2: Number of nodes $|\mathcal{M}_h(K)|$ and number of triangles $|\mathcal{B}_h(K)|$ in the surface discretization of the element in Figure 2 for different levels

the level $l = 0, 1, 2$. We recognize that in this situation much more trial functions and thus degrees of freedom are required in the global computations. Roughly speaking, the number of nodes doubles if the coarsest discretization of the faces is used. If a finer triangulation is needed, the number of nodes and thus the number of degrees of freedom increase ten times for $l = 1$ and even more than forty times for $l = 2$. Since the diameter of the elements are equal in all four situations, the approximation errors of the finite element computations are of the same order. Therefore, the method proposed in this manuscript is favourable because it has a smaller system matrix in the global finite element method. The dimension of this matrix is DoF $\times$ DoF, where DoF denotes the number of degrees of freedom which corresponds to $|\mathcal{N}_h|$ minus the nodes on the Dirichlet boundary Γ_D.
In the following, we investigate the influence of the face discretization. These triangulations of the faces are required to define the approximated trial functions $\psi_z^l \in \Psi_l$ on the faces with the help of local, two dimensional finite element methods. The finer the discretization is chosen the better we approximate the original trial functions $\psi_z \in \Psi_h$. Even though, the face discretization does not blow up the global system matrix, the computational effort for the local problems increases if the discretization level l is raised. As one example, we pick the element K from Figure 2 and list the number of nodes $|\mathcal{M}_h(K)|$ and the number of triangles $|\mathcal{B}_h(K)|$ in the surface discretization of K for different levels l in Table 2. We remember the dimensions of the matrices in the boundary element method which are given in (10). The main tasks in the local problems are the evaluation of the boundary element matrix entries and the inversion of the single layer potential matrix $\mathbf{V}_{K,h}$ which gives a local complexity of $\mathcal{O}(|\mathcal{B}_h(K)|^3)$.
In the next example, we analyse the rates of convergence for different values of l.

Example 1. Consider the Dirichlet boundary value problem

$$\begin{aligned} -\Delta u &= 0 \quad \text{in } \Omega = (0,1)^3, \\ u &= g_D \quad \text{on } \Gamma \end{aligned}$$

with $g_D = \gamma_0 u$ such that

$$u(x) = e^{2\sqrt{2}\pi(x_1-0.3)} \cos(2\pi(x_2-0.3)) \sin(2\pi(x_3-0.3)), \quad x \in \mathbb{R}^3$$

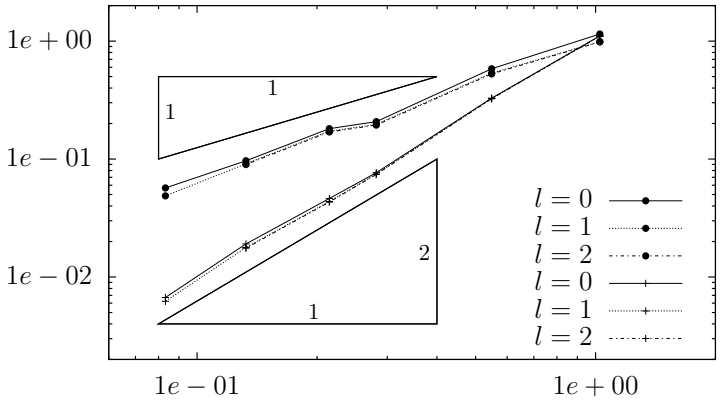

Figure 4: Relative error in $\|\cdot\|_E$ ($\bullet$) and $\|\cdot\|_{L_2(\Omega)}$ ($+$) with respect to h for $l = 0, 1, 2$ in Example 1 and triangles with slope one and two

is the exact solution. In Figure 4, the approximation errors $\|u - u_h\|_E$ and $\|u - u_h\|_{L_2(\Omega)}$ are given with respect to $h = \max\{h_K : K \in \mathcal{K}_h\}$ in a logarithmic plot for different discretization levels $l = 0, 1, 2$ of the faces.

This example shows that the discretization level of the faces does not influence the rates of convergence as we expect from the theory in Section 4. Therefore, the coarsest face discretization with $l = 0$ is sufficient to analyse the convergence rates in the forthcoming numerical experiments. Due to this choice, the local complexity in the two dimensional finite element method on the faces $F \in \mathcal{F}_h$ and the local boundary element methods on the elements $K \in \mathcal{K}_h$ is rather small. Furthermore, in Figure 4, we recognize linear convergence for the approximation error measured in the energy norm and quadratic convergence if the error is measured in the L_2-norm. This is the first numerical experiment in three space dimensions which confirms the rates of convergence for the BEM-based finite element method on Voronoi meshes with polyhedral elements and arbitrary polygonal faces.
Beside the Dirichlet problem for the Laplace equation, we also give examples for the Poisson problem and the case of a non-constant material parameter.

Example 2. The function $u(x) = \cos(\pi x_1)\sin(2\pi x_2)\sin(3\pi x_3)$, $x \in \mathbb{R}^3$ fulfills the boundary value problem

$$\begin{aligned} -\Delta u &= f \quad \text{in } \Omega = (0,1)^3, \\ u &= g_D \quad \text{on } \Gamma \end{aligned}$$

with $f = 14\pi^2 u$ and $g_D = \gamma_0 u$ fixed. In Figure 5, the errors $\|u - u_h\|_E$ and $\|u - u_h\|_{L_2(\Omega)}$ are shown with respect to $h = \max\{h_K : K \in \mathcal{K}_h\}$ in logarithmic scale.

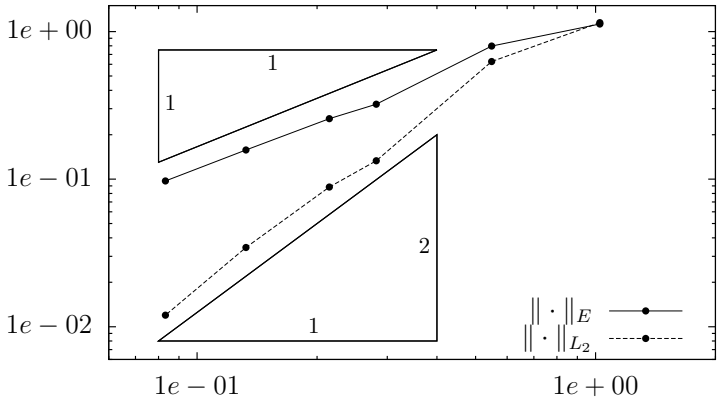

Figure 5: Relative error with respect to h for Example 2 with $l = 0$ and triangles with slope one and two

Example 3. We take the two functions already considered in Example 1 and 2 and label them by u_1 and u_2, respectively. They fulfill the boundary value problems

$$-\mathrm{div}\left((\tfrac{7}{2} - x_1 - x_2 - x_3)\nabla u_i\right) = f_i \quad \text{in } \Omega = (0,1)^3,$$
$$u_i = g_{iD} \quad \text{on } \Gamma$$

for $i = 1, 2$, where f_i and g_{iD} have to be chosen appropriately. In Figure 6, the approximation errors $\|u_i - u_{ih}\|_E$ and $\|u_i - u_{ih}\|_{L_2(\Omega)}$ are shown with respect to $h = \max\{h_K : K \in \mathcal{K}_h\}$ in logarithmic scale for $i = 1, 2$.

In the final two examples, we have also obtained optimal rates of convergence for the finite element approximation which confirm the theoretical results of the previous section. The BEM-based FEM yields linear convergence in the energy norm and quadratic convergence in the L_2-norm.

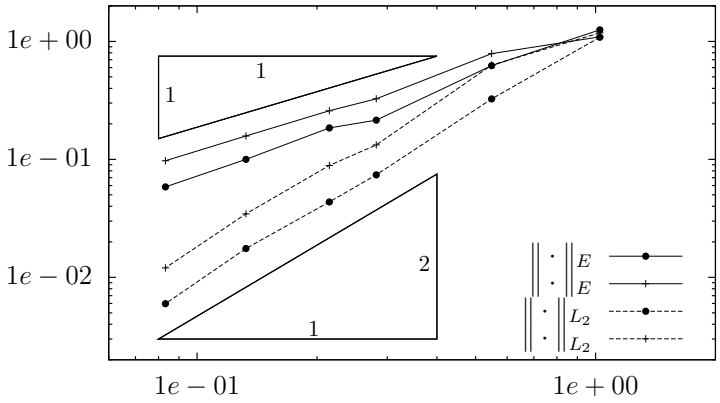

Figure 6: Relative error $\|u_i - u_{ih}\|$ for $i = 1$ ($\bullet$) and $i = 2$ ($+$) with respect to h for Example 3 and triangles with slope one and two

6 Conclusion

The classical convergence rates of finite element methods on simplicial meshes are recovered by the BEM-based FEM. However, the new methodology benefits from the flexibility with respect to arbitrary meshes with polyhedral elements having polygonal faces. This behaviour together with the conforming approximations makes the BEM-based finite element method an interesting and attractive strategy for ongoing research. Since the trial functions are defined in accordance with the underlying differential equation, the system of linear equations as well as the approximations contain already some information of the solution. This property is advantageous when considering other differential equations like convection-diffusion, for example, and it has to be investigated further.

References

[1] R. A. Adams. *Sobolev Spaces*. Academic Press, 1975.

[2] L. Beirão da Veiga, F. Brezzi, A. Cangiani, G. Manzini, L. D. Marini, and A. Russo. Basic principles of virtual element methods. *Math. Models Methods Appl. Sci.*, 2012. DOI: 10.1142/S0218202512500492.

[3] D. Braess. *Finite Elements*. Cambridge University Press, Cambridge, third edition, 2007. Theory, fast solvers, and applications in elasticity theory, Translated from the German by Larry L. Schumaker.

[4] S. C. Brenner and L. R. Scott. *The Mathematical Theory of Finite Element Methods*, volume 15 of *Texts in Applied Mathematics*. Springer, New York, second edition, 2002.

[5] F. Brezzi, K. Lipnikov, and M. Shashkov. Convergence of the mimetic finite difference method for diffusion problems on polyhedral meshes. *SIAM J. Numer. Anal.*, 43(5):1872–1896, 2005.

[6] V. I. Burenkov. *Sobolev spaces on domains*, volume 137. BG Teubner, 1998.

[7] P. G. Ciarlet. *The Finite Element Method for Elliptic Problems*. North-Holland, Amsterdam, 1978.

[8] D. Copeland, U. Langer, and D. Pusch. From the boundary element domain decomposition methods to local Trefftz finite element methods on polyhedral meshes. In *Domain decomposition methods in science and engineering XVIII*, volume 70 of *Lect. Notes Comput. Sci. Eng.*, pages 315–322. Springer, Berlin Heidelberg, 2009.

[9] D. M. Copeland. Boundary-element-based finite element methods for Helmholtz and Maxwell equations on general polyhedral meshes. *Int. J. Appl. Math. Comput. Sci.*, 5(1):60–73, 2009.

[10] V. Dolejší, M. Feistauer, and V. Sobotíková. Analysis of the discontinuous Galerkin method for nonlinear convection-diffusion problems. *Comput. Methods Appl. Mech. Engrg.*, 194(25-26):2709–2733, 2005.

[11] M. S. Ebeida and S. A. Mitchell. Uniform random voronoi meshes. In *Proceedings of the 20th International Meshing Roundtable*, pages 273–290. Springer, Berlin Heidelberg, 2012.

[12] M. S. Ebeida, S. A. Mitchell, A. Patney, A. Davidson, and J. D. Owens. A simple algorithm for maximal Poisson-disk sampling in high dimensions. *Comput. Graph. Forum*, 31, 2012.

[13] Y. Efendiev and T. Y. Hou. *Multiscale Finite Element Methods – Theory and Applications*, volume 4 of *Surveys and Tutorials in the Applied Mathematical Sciences*. Springer, New York, 2009.

[14] M. Floater, K. Hormann, and G. Kós. A general construction of barycentric coordinates over convex polygons. *Adv. Comput. Math.*, 24:311–331, 2006.

[15] A. Gillette, A. Rand, and C. Bajaj. Error estimates for generalized barycentric interpolation. *Adv. Comput. Math.*, 37:417–439, 2012.

[16] C. Hofreither. L_2 error estimates for a nonstandard finite element method on polyhedral meshes. *J. Numer. Math.*, 19(1):27–39, 2011.

[17] C. Hofreither, U. Langer, and C. Pechstein. Analysis of a non-standard finite element method based on boundary integral operators. *Electron. Trans. Numer. Anal.*, 37:413–436, 2010.

[18] K. Lipnikov, M. Shashkov, D. Svyatskiy, and Yu. Vassilevski. Monotone finite volume schemes for diffusion equations on unstructured triangular and shape-regular polygonal meshes. *J. Comput. Phys.*, 227(1):492–512, 2007.

[19] W. C. H. McLean. *Strongly elliptic systems and boundary integral equations*. Cambridge University Press, Cambridge, 2000.

[20] S. E. Mousavi and N. Sukumar. Numerical integration of polynomials and discontinuous functions on irregular convex polygons and polyhedrons. *Comput. Mech.*, 47:535–554, 2011.

[21] S. Rjasanow and S. Weißer. Higher order BEM-based FEM on polygonal meshes. *SIAM J. Numer. Anal.*, 50(5):2357–2378, 2012.

[22] O. Steinbach. *Numerical approximation methods for elliptic boundary value problems: finite and boundary elements*. Springer, New York, 2007.

[23] N. Sukumar and A. Tabarraei. Conforming polygonal finite elements. *Internat. J. Numer. Methods Engrg.*, 61(12):2045–2066, 2004.

[24] S. Weißer. Residual error estimate for BEM-based FEM on polygonal meshes. *Numer. Math.*, 118(4):765–788, 2011.